Changes in Halogen (F, Cl, Br, and I) and S Ratios in Rock-Forming Minerals as Monitors for Magmatic Differentiation, Volatile-Loss, and Hydrothermal Overprint: The Case for Peralkaline Systems

Hans G.M. Eggenkamp [1,*] **, Michael A.W. Marks** [1] **, Petya Atanasova** [1,2] **, Thomas Wenzel** [1] **and Gregor Markl** [1]

[1] Department of Geosciences, Eberhard-Karls-Universität Tübingen, Schnarrenbergstraße 94-96, D-72076 Tübingen, Germany; michael.marks@uni-tuebingen.de (M.A.W.M.); p.atanasova@hzdr.de (P.A.); thomas.wenzel@uni-tuebingen.de (T.W.); gregor.markl@uni-tuebingen.de (G.M.)

[2] Helmholtz-Zentrum Dresden—Rossendorf, Helmholtz Institute Freiberg for Resource Technology, 09599 Freiberg, Germany

* Correspondence: hans@eggenkamp.info

Abstract: We determined the halogen (F, Cl, Br, and I) and sulfur (S) concentrations in Cl-rich rock-forming minerals from five peralkaline complexes. We investigated sodalite (N = 42), eudialyte-group minerals (N = 84), and tugtupite (N = 8) from representative rock samples derived from Ilímaussaq (South Greenland), Norra Kärr (Sweden), Tamazeght (Morocco), Lovozero, and Khibina (Russian Federation). Taken together, sodalite and eudialyte-group minerals dominate the Cl and Br budget of the investigated rocks. For F, however, several other phases (e.g., amphibole, fluorite, villiaumite, and minerals of the rinkite group and the apatite supergroup) are additional sinks, and parts of the S may be scavenged in generally rare sulfides. The investigated minerals contain Cl at the wt.% level, F and S concentrations are in the hundreds to thousands of μg/g-range, Br is less common (0.2–200 μg/g) and I is rare (mostly well below 1 μg/g). Normalized to Cl, sodalite prefers Br relative to eudialyte-group minerals, while F is always enriched in the latter. Our data show that both F and S may represent important components in eudialyte-group minerals, sometimes at similar levels as Cl, which normally dominates. Sulfur reveals redox-dependent behavior: Under reduced crystallization conditions, S is more compatible in eudialyte-group minerals (EGM) than in sodalite, which flips to the opposite under water-rich and presumably more oxidized conditions. We investigate the applicability of F/Cl, Br/Cl, and S/Cl ratios in these minerals in peralkaline systems to better understand the interplay of magmatic differentiation, fluid loss and hydrothermal overprint. Similar to apatite in metaluminous systems, fractionation of sodalite, and eudialyte-group minerals in peralkaline magmas leads to decreasing Br/Cl ratios. The data presented in this study bear implications for the mineral chemistry and compositional variation of sodalite and especially EGM in general. Volatile components in EGM that are not normally considered, such as F and S, can reach concentrations of thousands of μg/g. Especially in the case of F, with its low atomic weight, the results obtained in this study indicate that it is very significant for formulae calculations, neutral charge-balance, and similar aspects at such concentration levels. This study demonstrates that halogen contents and ratios are sensitive monitors for a variety of processes in magmatic-hydrothermal systems, including magmatic fractionation, volatile loss, and fluid–rock interaction.

Keywords: eudialyte group minerals; sodalite; tugtupite; chloride; fluoride; bromide; sulfur; peralkaline rocks; Ilímaussaq

1. Introduction

Understanding the behavior of halogens in magmatic processes is essential for estimating global halogen budgets and exchanges between the different Earth system reservoirs. The role of magmatism in mediating halogen fluxes between these reservoirs is important for several reasons, including their capacity for transporting metals in fluids (e.g., in ore-forming processes) and their environmental impact on the atmosphere during magmatic degassing and fluid exsolution [1,2]. Besides H_2O, CO_2, and S, halogens are important components of magmatic fluids and volcanic gases. Although F and Cl are normally dominating, Br and I are significant components in volcanic gases [3–5], and it was demonstrated that Br species in the stratosphere are notably involved in the destruction of ozone, being much more efficient than Cl in this respect [6]. The importance of I, however, is very poorly known. Thus, as recently pointed out [2], the understanding of the geochemical cycle of the less abundant halogens Br and I [7] and establishing reliable analytical methods for their determination in geological materials [8–12] are important challenges.

Silicate magmas can dissolve significant amounts of halogens, depending on several factors, such as pressure (P), temperature (T), H_2O content, and major element composition. For example, the solubility of F in rhyolitic melts reaches 8 wt% [13–15] and reach similar levels in phonolitic compositions [16]. The solubility of Cl increases with increasing peralkalinity and FeO* content but decreasing SiO_2 content and may reach about 0.8–0.9 wt.% [16–19]. Due to gravitational separation of minerals after they are crystallized from the melt, whole rock Cl contents can show significantly increased values in rocks where sodalite with its low density compared to other minerals is cumulated. Similarly, Br solubility depends on several factors, reaching >1 wt.% in peralkaline compositions [20]. In melt-fluid systems, the heavier halogens (Cl and Br) preferentially partition into the fluid phase, whereas F is largely retained in the melt [14,21–24]. Magmatic degassing fractionates Cl from Br, as the KD fluid/melt value for Br is about two-fold higher compared to that of Cl (about 18 versus about 9) [20,21]. Thus, fluid exsolution in magmatic systems influences F/Cl and Cl/Br ratios in residual magmas.

In rock-forming minerals, the relatively small F^- ion (133 pm) can easily substitute for OH^- (132–137 pm [25]), and therefore behaves only moderately incompatible during magmatic differentiation. In contrast, the heavier halogens Cl^- (181 pm) and Br^- (195 pm) show stronger incompatible behavior during magmatic differentiation, probably a consequence of their larger ionic radii [2,26]. The most common halogen-bearing minerals in magmatic rocks are apatite, mica, and amphibole, besides accessory titanite, fluorite, or topaz. In most magmatic rocks, apatite, mica, and amphibole are generally F-rich and relatively Cl-poor [27–29], as mineral-melt partition coefficients for F are generally >1, whereas those for Cl are mostly <1 [28–30]. Because of its low abundance and analytical difficulties, relatively few Br data are available for magmatic minerals [9,31–36]. In general, Br contents in apatite, mica and amphibole are low (mostly <5 μg/g) and Br/Cl ratios in apatite are usually lower than those of associated amphibole and biotite [24,29,37–39]. Consequently, Cl/Br ratios of magmas may change during magmatic differentiation, depending on the amount and the halogen composition of the fractionating phases. In all, the high solubility of F, Cl, and Br in silicate magmas and their variable behavior during mineral-melt and fluid-melt partitioning renders them ideal tracers for various magmatic and hydrothermal processes, such as magmatic differentiation, fluid exsolution and fluid/rock interaction [21,23].

Peralkaline igneous rocks (rocks with a molar (Na + K)/Al ratio >1) are strongly enriched in halogens (F, Cl, Br, and I), and because of their high levels of high field strength elements (HFSE; such as Zr, Hf, Nb, Ta, and U and the rare earth elements (REE)); they are of large economic interest [40–42]. Their halogen-rich nature results in the formation of abundant halogen-rich minerals (see Table 1), including F-minerals (fluorite and villiaumite), Cl-minerals (sodalite and tugtupite), and various halogen-bearing Na-Ca-HFSE minerals that are either F-rich or Cl-rich, the most common of them being eudialyte-group minerals (EGM).

Table 1. Most common F^{−} and Cl^{−} bearing minerals in peralkaline systems. Eudialyte and kentbrooksite (*) are sometimes considered two endmembers of the eudialyte group, where eudialyte (*) is the Si, Fe, Cl and kentbrooksite the Nb,Mn,F endmember.

Mineral Name	Formula
Fluorite	CaF_2
Villiaumite	NaF
Rinkite	$(Ca_3REE)Na(NaCa)Ti(Si_2O_7)_2(OF)F_2$
Wöhlerite	$Na_2Ca_4Zr(Nb,Ti)(Si_2O_7)_2(O,F)_4$
Natrophosphate	$Na_7(PO_4)_2F.19H_2O$
Vuonnemite	$Na_6Na_2Nb_2Na_3Ti(Si_2O_7)_2(PO_4)_2O_2(OF)$
Kentbrooksite *	$Na_{15}Ca_6Mn_3Zr_3NbSi(Si_{24}O_{73})(O,OH,H_2O)_3(F,Cl)_2$
Eudialyte *	$Na_{15}Ca_6Fe_3Zr_3Si_2(Si_{24}O_{73})(O,OH,H_2O)_3(Cl,F,OH)_2$
Sodalite	$Na_8Al_6Si_6O_{24}Cl_2$
Tugtupite	$Na_4BeAlSi_4O_{12}Cl$

The presence of the latter (halogen-bearing Na-Ca-HFSE minerals such as eudialyte group minerals) defines so-called agpaitic rocks [43–47]. Sodalite and EGM represent by far the most important sinks for Cl and Br in peralkaline rocks [33,48–51]. Both are stable over a very long crystallization interval: They form at T > 800 °C [16,52] and are known to form during late-magmatic and hydrothermal stages as well [47]. As both minerals are Cl-rich, their fractionation during magmatic differentiation processes should impact F/Cl, Br/Cl, and I/Cl ratios in evolving magmatic to hydrothermal systems [16,53,54]. However, concentration data of F, Br, and I for sodalite and EGM to test this are very limited: Sodalite contains Br at the tens to hundreds of μg/g-level [33,53–55], the only published data for EGM to date indicate Br contents on the order of 7 μg/g [39]. No systematic concentration data for F and I in sodalite and EGM exist.

This study documents halogen (F, Cl, Br, and I) and S concentrations in a set of well-characterized sodalite- and EGM-bearing rocks from the Ilímaussaq complex (South Greenland) and compares these data with similar rocks from Norra Kärr (Sweden), Tamazeght (Morocco), Lovozero, and Khibina (Russian Federation). These data are used to investigate the potential of sodalite and EGM to monitor magmatic and hydrothermal processes and to characterize the behavior of halogens in peralkaline systems in more detail.

2. Sample Material and Geology

The studied samples derive from five peralkaline intrusions: Ilímaussaq (South Greenland), Norra Kärr (Sweden), Tamazeght (Morocco), Lovozero, and Khibina (Russian Federation). These intrusions have different characteristics and we anticipate that this will allow us to differentiate between processes that are specific for the individual minerals and those that are specific for the different intrusions, which may derive from different parental melt compositions. For example, Ilímaussaq rocks contain abundant orthomagmatic sodalite and EGM, whereas in Tamazeght, sodalite, and EGM formed only locally during late-magmatic stages. Norra Kärr consists of deformed and metamorphosed EGM-bearing rocks that lack sodalite. For Ilímaussaq and Norra Kärr, alkali basaltic parental melts are assumed, whereas Khibina, Lovozero, and Tamazeght probably derived from (mela-)nephelinitic parental magmas [47,56–60].

The major focus of this study lies on the Ilímaussaq intrusion, which is the best studied of all alkaline intrusions (see recent review [61]). For this study we included 127 mineral separates (35 sodalite, 84 EGM, and eight tugtupite samples) for which the mutual textural relationships are well understood. These samples cover the entire exposed stratigraphic sequence of the intrusion and include orthomagmatic and hydrothermal samples. For comparison, we added six samples from Tamazeght (one sodalite and five EGM), 7 EGM from Norra Kärr, 11 EGM from Lovozero, and seven EGM from Khibina covering the major EGM-bearing lithologies. In the following, brief overviews on the geology of the five investigated localities are presented.

2.1. Ilímaussaq (Southwest Greenland)

The Mid-Proterozoic Ilímaussaq complex represents a textbook example for the evolution of peralkaline magmas, culminating in some of the geochemically most evolved rocks known on Earth. A review of the present knowledge on the origin and evolution of the Ilimaussaq magmatic system has been published recently [61]. In short, the magmas forming the complex were derived from partial melting of an isotopically homogeneous, but metasomatically enriched mantle source, resulting in an alkali basaltic parental magma. The complex is dominated by several types of agpaitic foid syenites that are linked to each other by extensive m agmatic differentiation during low oxygen fugacity and water activity. The unusual composition of the magma and the extreme physico-chemical conditions during their crystallization allowed for the large-scale formation of orthomagmatic, late-magmatic, and hydrothermal sodalite-EGM assemblages and the retention of aqueous fluids to a very late stage [62,63]. Studies focusing on non-traditional stable isotopes (Li and Fe) showed that extensive magmatic differentiation produces significant isotopic fractionation between minerals of the various rock units as well as between different minerals of the same rock type [64,65]. Late-stage fluid exsolution even resulted in the isotope fractionation of heavy elements such as Tl [66].

The agpaitic suite of the Ilímaussaq intrusion has a layered structure and consist of coarse-grained roof series (mainly sodalite foyaites and naujaites) and floor series (kakortokites) cumulate rocks and fine-grained and melanocratic rocks (lujavrites) that possess strong magmatic fabrics. These lujavrites intrude the roof series rocks, but seemingly evolve out of the floor series rocks. Sodalite foyaites, naujaites, kakortokites, and lujavrites are mineralogically rather similar but the textures and modal amounts of sodalite and EGM are distinct. In sodalite foyaites, and especially in naujaites, euhedral sodalite is very abundant (up to 70 vol.%), while EGM is interstitial and less frequent than sodalite (5–35 vol%.); kakortokites contain abundant euhedral EGM but much less sodalite; lujavrites contain variable but comparably minor amounts of euhedral sodalite and/or EGM. The agpaitic suite contains abundant hydrothermal veins that are mineralogically diverse. Some of them contain abundant sodalite and tugtupite (for details see in [61] and the references therein).

2.2. Tamazeght (Morocco)

This Eocene composite magmatic complex contains a large variety of alkaline rock types (including pyroxenites, glimmerites, gabbroic to monzonitic rocks, syenites, nepheline syenites, and carbonatites) and documents a progression from ultramafic to felsic alkaline magmatism [67]. Simple fractional crystallization is not a likely mechanism to explain the large variety of lithologies present in the Tamazeght complex. It is most probable that successive melting of a compositionally heterogeneous mantle source region gave rise to several melt batches with distinct compositional and physicochemical characteristics (for details see in [68–71]). Based on detailed petrographic and mineral chemical data, the various units crystallized under markedly different redox conditions and these parameters influence both the phase assemblage and their detailed chemical evolution, including their halogen contents [39,68]. Orthomagmatic sodalite is a minor phase only in some of the gabbros, monzonites, syenites and nepheline syenites [68]. Late-magmatic to hydrothermal sodalite-EGM assemblages occur irregularly dispersed in several spatially restricted areas within an otherwise and sodalite-poor and EGM-free nepheline syenite body [47,72].

2.3. Lovozero and Khibina (Russian Federation)

These alkaline complexes represent two of the largest peralkaline intrusive complexes on Earth, with about 600 and even 1300 km^2 outcrop size respectively. They are spatially closely correlated and part of the Devonian Kola Alkaline Province. Within this igneous province, they represent some of the most differentiated members and consist of variably evolved peralkaline rocks (mostly syenites and nepheline syenites) and minor amounts of carbonatites and ultramafic rocks [73,74]. Structurally, both complexes bear similarities with Ilímaussaq. They are multiphase intrusions, and partly consist

of distinctly layered sections [75]. The parental magmas for these complexes are assumed to be (mela)nephelinitic to melilititic [59]—very different from Ilímaussaq and Norra Kärr, for which alkali basaltic parental magmas are likely. Thus, the differentiation path before reaching the peralkaline stage did probably not involve large amounts of plagioclase fractionation, which is now monitored by compositional differences in EGM [76]. Sodalite and EGM occur in many of the Lovozero and Khibina rocks but are much less common than in most Ilímaussaq rocks. Especially at Khibina they are largely restricted to late-magmatic and hydrothermal conditions, while orthomagmatic sodalite-EGM assemblages are relatively rare. Furthermore, the mineral assemblages are slightly different compared to many Ilímaussaq rocks, indicating less halogen-rich magma compositions and less reduced crystallization conditions for the Khibina rocks [73,77].

2.4. Norra Kärr (Sweden)

This Meso-Proterozoic intrusion represents one of the very few known examples of deformed and metamorphosed EGM-bearing rocks, which were affected by the Sveconorvegian orogeny about 350 Ma after their magmatic emplacement [78]. The deformation textures in the rocks vary systematically, culminating in migmatite-like schlieren in the rocks of the central part of the complex, suggesting partial melting [78]. Based on detailed petrography and electron microprobe work, it was possible to distinguish magmatic and metamorphic processes in the complex and link systematic compositional changes of clinopyroxene and EGM to magmatic differentiation and subsequent metamorphic overprint [58].

In contrast to most other EGM-bearing rocks, the lithologies of the Norra Kärr complex are sodalite-free and other potentially Cl- and Br-bearing minerals (e.g., amphibole, mica, and apatite) are only very minor constituents. Thus, EGM is the dominating Cl and Br host for the complex. By comparison with the other intrusions studied here this offers the possibility to study the behavior of the halogens during (i) magmatic differentiation without the presence of sodalite and can be used to explore the potential influence of (ii) fluid-assisted metamorphic overprint and (iii) partial melting.

3. Methods

Mineral separates of sodalite, tugtupite and EGM were produced by crushing and sieving rock samples and subsequent standard magnetic and (halogen-free) heavy liquid (sodium polytungstate solutions) separation techniques. From these first concentrates, high-purity concentrates were produced by hand-picking under the binocular. These concentrates where powdered by hand-milling in an agate mortar.

Bulk halogen (F, Cl, Br, and I) and S analyses were done by Combustion Ion Chromatography (CIC) using a 930 Metrohm Combustion IC PP. This is an integrated system consisting of an Auto Boat Driver (autosampler) and Combustion Module by Analytik Jena and a 920 Absorber Module and 930 Compact IC Flex by Metrohm. The setup is basically a pyrohydrolysis system that combusts a sample and the evaporated species are transported in a water flow and trapped into an absorber solution. For combustion, a small sample (5 to 10 mg) is weighted and mixed with an equivalent amount of WO_3 flux into a quartz vial (6×18 mm), which is closed on both ends with a small wad of Tosoh quartz wool fine grade. The vial is placed into a quartz boat that is fed through the autosampler into the combustion module. Here, the sample is combusted at 1050 °C for 12 min in a flow of O_2 (5.0; 300 mL/min) and Ar (6.0; 100 mL/min), while a constant water flow (0.2 mL/min) is maintained. The loaded steam is collected in the absorber module, where it is trapped into about 5 mL of a 450 mg/L H_2O_2 solution. This solution is then transferred to the 930 Compact IC flex and injected onto the ion chromatographic column.

This separation column is a Metrohm Metrosep A Supp 5-250/4.0 column that separates the negative ions from each other based on mass and ionic charge. Besides the analytes of interest (F^-, Cl^-, Br^-, I^-, and SO_4^{2-}) further anions were detected (NO_3^-, PO_4^{3-}, and WO_4^{2-}). Of these, WO_4^{2-} originates from WO_3 added as flux to the sample (see above). Further, it is known that PO_4^{3-} does not escape completely during pyrohydrolisis at 1050 °C, which results in measured concentrations

that are significantly lower than the actual concentrations, and as such it is not representative of the actual concentration in the sample. N in rocks is mainly present in the form of ammonium (NH_4^+), and the measured NO_3^- is likely to reflect NH_4^+ from the sample that is oxidized to NO_3^- during combustion [79–81]. As the chemistry of N in magmatic rocks is poorly understood and not part of our current investigation, NO_3^- is not taken into consideration at this stage. Each sample is eluted over the IC column following a procedure developed by Walter [82] using an 8 mM Na_2CO_3 eluent, while the column is kept at 40 °C. The whole system is automated and controlled by the MagIC software (Metrohm).

For calibration and quantification, primary reference solutions were prepared by mixing single anion-solutions (Roth; 1000 mg/L) and except for F, a calibration curve that covered the full concentration range investigated was constructed. These calibration curves could either be a power function (concentration = a × peak_area^b), or a second order polynomial function (concentration = a × peak_area^2 + b × peak_area + c), whatever fitted best depending on the measurements of the standards over the ten-month period that the samples were measured.

In the ion-chromatography column, fluoride behaves considerably different from the other anions in the Cl-rich solutions that were analyzed. This behavior complicates the measurement and calibration of fluoride considerably. The peak area at a given F concentration decreases significantly when Cl/F ratios in the solution exceed values of about 10 (Figure 1). For example, for 0.1 mg/L F (dark blue curve in Figure 1), the peak area for F is about 0.35 for Cl/F ratios ≤1 but decreases strongly to 0.042 (almost ten times smaller) at Cl/F ratios above 3000. As the Cl/F ratios in Cl-rich minerals analyzed in this study varies considerably, reference solutions with variable F concentrations (0.01–10 mg/L) and Cl/F ratios (0.04–3000) were prepared to resolve this dependency and manually correct for it accordingly. The reason for this effect may be the relatively short analysis time of only 25 min. We anticipate that when the size of the Cl peak increases considerably it pushes the F peak ahead, partly into the negative water peak just before the F peak in the chromatogram. This effect may increase in importance when the Cl peak is larger and is significant in our measurements as the Cl concentration in sodalite is higher than in EGM. The F peak is much smaller for sodalite samples than for EGM samples, while, after correction F concentrations in sodalite and EGM samples do not show large differences. The correction of the F concentration for the Cl/F ratio of the peak areas thus is very important to apply here.
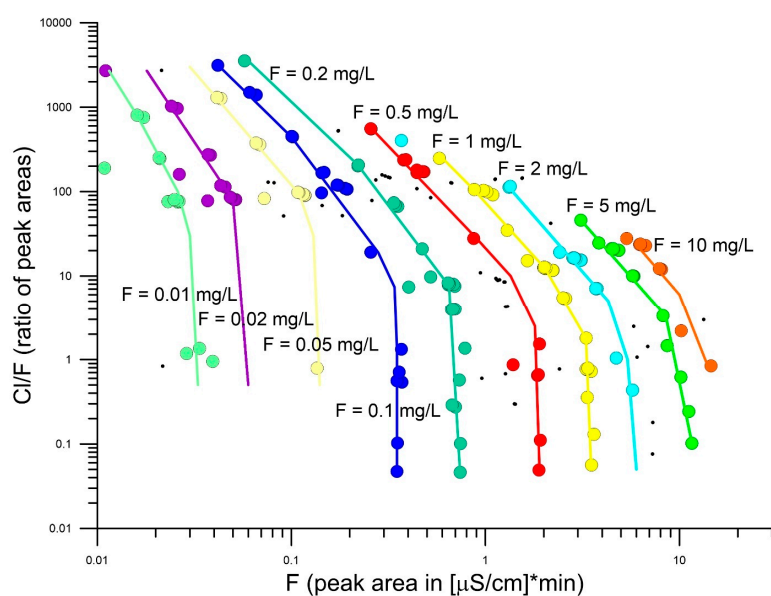

Figure 1. Relationship between F^- peak area, Cl/F peak area ratio and the F^- concentration of standard solutions with different Cl^- concentrations. At high Cl^- concentrations the F^- peak area decreases significantly, suggesting apparently lower F^- present in the sample than is actually present. Small black dots indicate intermediate, additional (not 1, 2, or 5) F concentrations used for calibrating the F concentrations.

In all, the effective detection limits for powdered samples were about 20 µg/g for F in sodalite and tugtupite samples, 5 µg/g for F in EGM samples, about 10 µg/g for Cl, 1 µg/g for S and about 0.2 µg/g for Br and 0.1 µg/g for I. Based on the frequent analyses of standard solutions and various reference materials, relative uncertainties were generally <10% (1σ level) for F, Cl, and S, and up to ~20% for Br. I is regularly very close to the detection limit and relative uncertainties can be larger than 50%. Relative uncertainties are depending on the concentrations of the analytes (i.e., are in general smaller at higher concentrations).

4. Results

Halogen and S concentration data for EGM, sodalite, and tugtupite are summarized in Supplementary Tables S1 and S2. Uncertainties shown indicate one standard deviation for replicate measurements (usually two); in cases where no uncertainty is given, only one measurement could be done.

4.1. Eudialyte-Group Minerals

For EGM, bulk Cl contents vary largely between about 0.1 and 1.8 wt.%, with the lowest values for samples from Norra Kärr. Compared to published Electron Probe Micro-Analyzer (EPMA) data [48,49,58,72,83,84], most CIC data overlap within a 20% uncertainty (Figure 2).
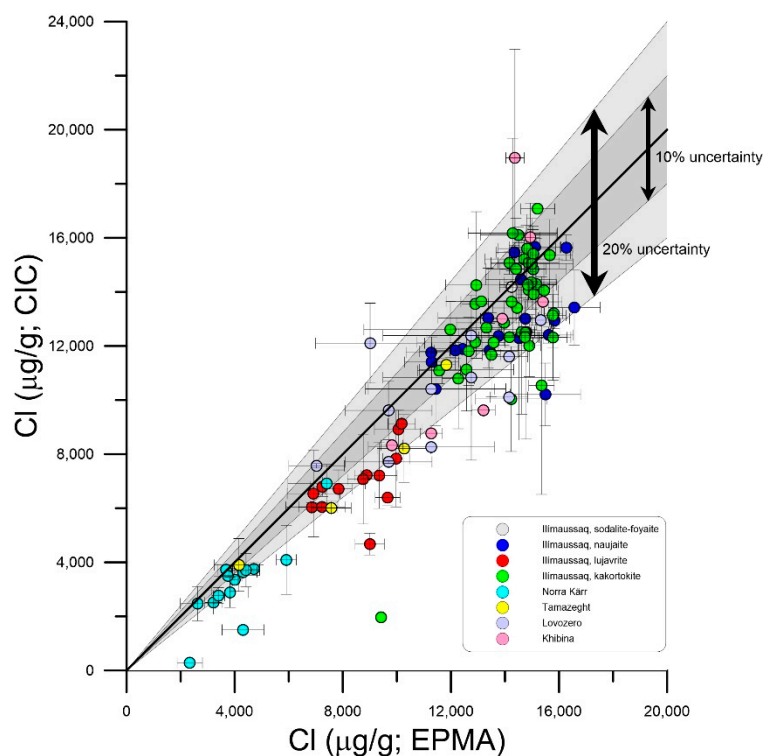

Figure 2. Comparison between Cl concentrations in eudialyte-group minerals (EGM) measured by Combustion Ion Chromatography (CIC) (bulk) and EPMA (spatially resolved), with 10% and 20% uncertainty envelopes. Strong deviations between the two methods indicate impurities in hand-picked mineral separates. Samples outside the 20% uncertainty range have not been considered further in the discussions in this paper.

Note that the relatively large range of EPMA data for some of the samples are due to compositional zonations of EGM in individual crystals, which is not mirrored in the CIC data, as these represent bulk samples (about 5 mg, see above). Some CIC data are, however, lower than the corresponding EPMA data. This is probably caused by impurities in the hand-picked separates that mostly consist

of halogen-free minerals, such as clinopyroxene, nepheline, albite, and zeolites. These occur as small inclusions or as alteration minerals in EGM and sodalite. As these impurities influence the other analytes (F, Br, I, and S) as well, we omit EGM data with deviations larger than 20% from further discussion.

Results from the EGM are summarized in Figure 3. Results from Ilímaussaq are ordered stratigraphically. Ilímaussaq is a classic example of a layered intrusion and it is common practice to present data from this complex in stratigraphic order (see, e.g., in [61] and other chapters in this book). Samples from the other intrusions are randomly ordered.
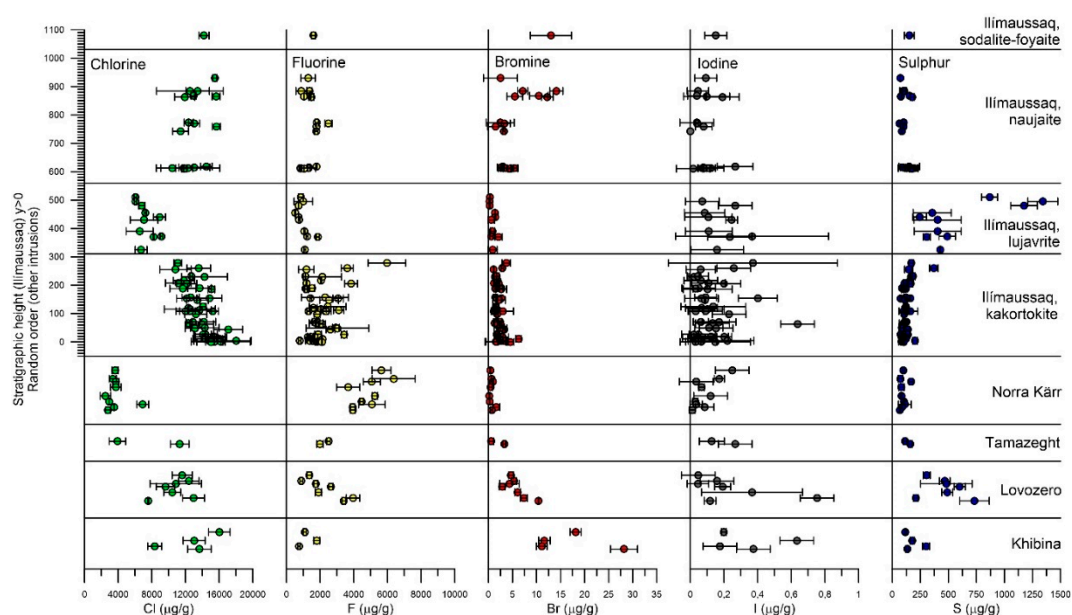
Figure 3. Halogen (Cl, F, Br, and I) and S concentrations in EGM based on CIC measurements. Ilímaussaq samples are sorted according to their stratigraphic height in this intrusion, samples from the other four intrusions are randomly ordered.

Fluorine contents are particularly interesting as F is normally not analysed by electron microprobe because of different interferences that cause high detection limits at about 0.1 to 0.15%. Our data reveal significant and variable F contents in EGM. They are highest and most variable in floor cumulates (ranging from less than 1000 to above 3000 μg/g, with the highest values, up to 4000 μg/g, in the uppermost floor cumulates), lower in the roof cumulates (up to about 2000 μg/g) and lowest in the evolved lujavrites (between 500 and 1000 μg/g). In Norra Kärr F is mostly higher than Cl. F varies between 3000 and 9000 μg/g, and because Cl is mostly low in this intrusion F/Cl can be higher than 2 indicating that F in apfu is higher than Cl. In Tamazeght, Lovozero, and Khibina, the F contents are more in line with F in Ilímaussaq.

Bromine contents in EGM are highest in the roof cumulates where they decrease downwards the stratigraphy from up to 14 μg/g to values of around 5 μg/g (Br/Cl × 1000 from about 1 down to 0.3). In floor cumulates, Br contents broadly decrease from about 4 μg/g in the lower samples to about 1 μg/g in the upper samples (Br/Cl × 1000 from about 0.3 down to 0.05), with similar positive excursions in some of the uppermost kakortokites, as observed for F. In lujavrites, Br is even lower (between 2 and 0.2 μg/g). Iodine contents are very low (≤0.5 μg/g) in all EGM samples and most values are close to the established detection limit of about 0.1 μg/g (see above). In most Norra Kärr samples Br is very low. One sample (NK 5613) however shows an extremely high amount of Br (481 μg/g). In Tamazehgt and Lovozero Br is in line with Ilímaussaq, while in Khibina the Br contents are mostly higher than in Ilímaussaq.

Sulfur contents are highly variable (mostly between 50 and 500 µg/g), which translates to a maximum of 0.15 apfu, demonstrating that S can be an important component in EGM. While S in roof and floor cumulates is relatively low (mostly 50–200 µg/g), lujavrites are S-rich, with the most extreme values of about 1250 µg/g. S is variable in the other four intrusions. It is lowest in Norra Kärr (50 to just over 100 µg/g), higher in Tamazeght and Khibina (about 100 to 300 µg/g) and highest in Lovozero (mostly above 300 µg/g). Very little is known of the behavior of S in EGM. Rastsvetaeva [85] describes one specimen in which S is contained at the M(3) location in the EGM lattice and another in which it is on the X(1) location. In their classification of eudialyte-group minerals, Rastsvetaeva & Chukanov [86] only suggest that SO_4 can be one of the ions that fits on the locations X(1) or X(2) in the eudialyte crystal. Sulfur is most probably present as sulfate in EGM, which in the case of Ilímaussaq is confirmed by our observations on EGM where we did not observe either the smell of sulfide or a black Ag_2S precipitate upon dissolution and subsequent precipitation of chloride for Cl isotope analysis preparations. Recently [87], the first EGM showing substitution of chloride by sulfide was described. In their specimen about 0.5 apfu S^{2-} is present at the Cl location. This observation shows that sulfur can be present in the form of different species, at the very least as sulphate or sulfide. During CIC analysis however all S-species are oxidized to sulfate and we report the S content in our samples as total S (Figure 2).

4.2. Sodalite

Due to low sodalite contents in intrusions other than Ilímaussaq it was only possible to measure a single sodalite sample from Tamazeght and none from the other intrusions. In Ilímaussaq, sodalite in roof and floor cumulates is known to be close to the Cl-endmember composition [33,54,88], containing around 7 wt.% Cl. Most of the bulk sodalite CIC data scatter around this value but some samples showed, however, much lower Cl contents. This is because of impure concentrates, because sodalite in most of these samples is rather fine-grained and intergrown with Cl-free minerals (such as albite, nepheline and zeolithes) that are not easily separated from sodalite and occur in these samples to variable amounts [63]. The apparently low Cl values for these samples are therefore not considered further. Fluorine in magmatic sodalite from roof and floor cumulates (up to about 5000 µg/g), is much higher than in hydrothermal sodalite (mostly below 1000 µg/g). Similar to what was observed for EGM, Br contents in sodalite decrease downwards the roof cumulate sequence from about 150 to 50 µg/g and are low, at values below 40 µg/g in the floor cumulate sequence (Figure 4). Iodine contents in magmatic sodalite (mostly below 0.5 µg/g) are in most cases slightly higher than in EGM, in hydrothermal sodalite I variation is very largest, from samples with virtually no I to higher values of about 6 µg/g. Sulfur contents are higher in sodalite from the floor cumulates (900–1200 µg/g) than in those from roof cumulates (250–560 µg/g), hydrothermal sodalites show variable and partly very high S contents (up to about 5000 µg/g; Figure 4). The only sodalite sample from Tamazeght shows anion concentrations that are in line with those from Ilímaussaq.

4.3. Tugtupite

Tugtupite is only found in rocks from Ilímaussaq in this study.

Chlorine contents in the tugtupite samples determined by CIC are on average 5.2 wt.%, which is well below the expected value of 7.6 wt.% according to the ideal chemical formula. However, the samples are fresh and do not contain any obvious inclusions, as was the case for some of the sodalite samples. Rather, the presence of Be in tugtupite at the wt.% level [88] may explain this, as many Be compounds show covalent properties. If parts of the Cl are present after combustion as $BeCl_2$ or Be-Cl ionic complexes, this would result in an overall under determination of the actual Cl concentrations, as only chloride is detected during CIC. Although it is unclear to what extent the minor halogens (F, Br, and I) are influenced by such effects as well, but for example, possible BeI_2 that is formed during combustion may produce IO^- ions upon dissolution in water, and this may affect (decrease) the measured I contents in a sample. Thus, the determined contents of F (generally below

200 µg/g), Br (below 50 µg/g), I (below 0,5 µg/g), and S (mostly below 30 µg/g) contents are preliminary only and clearly, further research is necessary to evaluate these potential problems during analysis of tugtupite (and other Be-containing minerals) by CIC techniques.
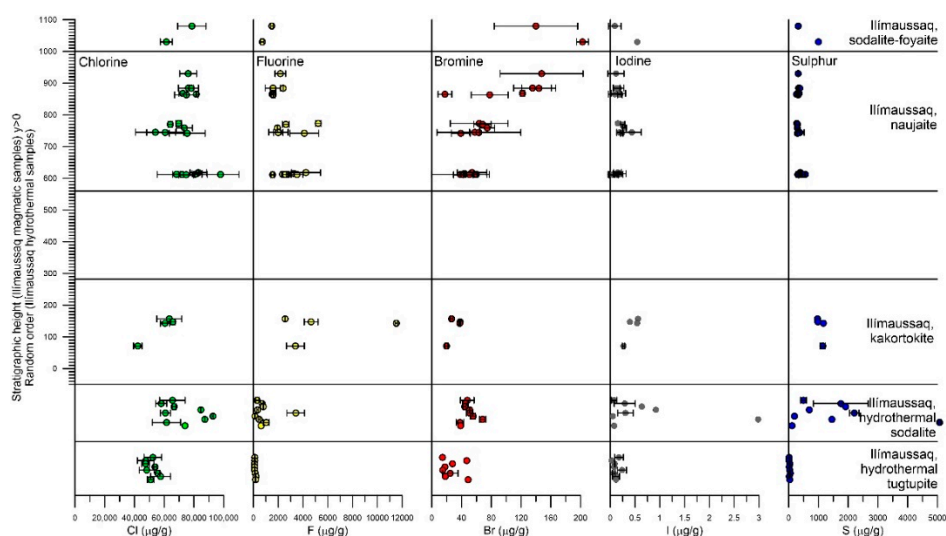

Figure 4. Halogen (Cl, F, Br, and I) and S concentrations in sodalite and tugtupite based on CIC measurements. Magmatic Ilímaussaq samples are sorted according to their stratigraphic height in the intrusion, other samples are randomly ordered within each group.

Literature data for F, Br, and I are absent for tugtupite. For S, rather old publications indicate S at the thousands of µg/g level [88,89], while modern studies [90,91] showed S to be below their respective detection limits of <50 and <5 µg/g, respectively. Moreover, a Wavelength-Dispersive Spectroscopy (WDS) scan for S in the tugtupite used as Cl standard at the electron microprobe facility at University of Tübingen revealed no detectable S, indicating that the apparently low S contents for the investigated samples are trustworthy. It was, however, suggested [92] that the reddish colour of tugtupite as well as its luminescence and tenebrescence could be ascribed to the presence of S^{2-} ions in the mineral. This suggestion was confirmed [90,91] although in both studies it is also suggested that the luminescence might be a composite effect of both S^{2-} ions and tetrahedral Fe^{3+} centers. Therefore, despite the very low S contents in these tugtupite samples the luminescence can still be the result of these very low amounts. In conclusion, the data presented [90,91] indicate that low S contents as observed in our present study are sufficient to explain luminescence and tenebrescence as observed in tugtupite.

Due to the potential and unexplained possible flaws in the measurements of the anions in tugtupite these data are not further considered in the discussion.

A visual illustration of the final data sets for EGM and sodalite is presented in Figures 3 and 4, where the samples from Ilímaussaq are plotted according to their stratigraphic position and samples from the other four locations are plotted in random order.

5. Discussion

Halogen and S contents and ratios (e.g., F/Cl, Br/Cl, I/Cl, and S/Cl) in minerals have been shown to monitor magmatic, hydrothermal, and weathering processes in granitic and hydrothermal ore systems [9,37,93–95]. In the following, it will be tested if this applies to for peralkaline systems as well. The samples from Ilímaussaq include orthomagmatic and hydrothermal samples that cover the exposed stratigraphic sequence of the intrusion and allow for investigating the behavior of halogens and S during the evolution of a peralkaline magmatic system in some detail, which will be discussed first. We then use samples from Tamazeght, Norra Kärr, Lovozero, and Khibina for comparison,

which enables us to characterize the diversity of halogen characteristics in peralkaline systems in a broader sense and test the suitability of these differences for deciphering different sources and differentiation histories.

5.1. Halogens in EGM and Sodalite from Ilímaussaq

5.1.1. Eudialyte Group Minerals

Consistent with previous work, Cl contents in EGM slightly decrease upwards in the floor cumulate section (kakortokites) from about 1.5 to 1.2 wt.% but are much lower in the lujavrite section (between 0.6 and 0.8 wt.%; Figure 3). This was explained by a successive increase of water activity during differentiation [49,96], which causes higher OH^- contents on the Cl site of the eudialyte crystal structure. A large change in water activity during formation of the floor cumulates seems unlikely because of petrological reasons (see details in [61]). Thus, the decreasing Cl contents in EGM from the kakortokite section is ascribed to decreasing Cl contents in the magma because of large-scale extraction of EGM and (simultaneous?) sodalite extraction during roof cumulate formation. Thereby, the Cl content of the melt decreases continuously since sodalite crystallizes with a stoichiometrically fixed amount of Cl (about 7 wt.%) (Figure 4). The Cl content in EGM appears to monitor this continuous decrease in Cl in the melt, in line with the Cl decrease in the melt towards lower temperatures [16].

Interstitial EGM in the roof cumulates have rather variable Cl contents that cover the range found in the floor cumulates, with no obvious trend along the stratigraphy.

Figure 5 shows the relationships between the Cl contents and the ratios between the measured anions (F, Br, I and S) for the different EGM measurements.

The Br/Cl ratios in EGM from the roof cumulates are highest and decrease downwards in the sequence from 1.1×10^{-3} to 0.2×10^{-3}. These rocks also contain large amounts of sodalite (that crystallized before EGM) with high Br contents (see above) and similarly decreasing Br/Cl ratios. We suggest that this reflects decreasing Br/Cl ratios in the evolving magma, while diffusional exchange of Br between sodalite and EGM remains to be tested. Decreasing Br/Cl ratios upwards in the floor cumulate sequence (from 0.4×10^{-3} to 0.07×10^{-3}) parallel such an evolution, although there is no clear dependency between Br/Cl and Cl concentration (Figure 5). Nevertheless, preferred extraction of Br relative to Cl during magmatic evolution seems plausible and the final evolved rocks (lujavrites) show indeed the lowest Br contents and Br/Cl ratios (0.2×10^{-3} to 0.04×10^{-3}) in EGM.

For F/Cl ratios, however, there is no clear variation along the stratigraphy, and these ratios mostly overlap between floor cumulates (0.08–0.54), roof cumulates (0.07–0.19), and the evolved lujavrites (0.07–0.23). Moreover, there is no clear relationship with Cl content, probably because the F budget in the investigated Ilímaussaq rocks is largely governed by amphibole that contains around 1 wt.% F [49,97] and minor/accessory fluorite and villiaumite (NaF). Until now, the F content of EGM has never been considered for the F budget of such rocks, as it was generally assumed that the F content in EGM is very low. Here we show, however, that F in EGM is significant (0.1 to 0.3 wt.%). Considering the high modal EGM content in some of the investigated rocks, a significant part of F will be present in EGM and thus cannot be ignored when discussing the F budget in EGM-rich systems. This is especially important for rocks from Norra Kärr (see details below).

The I/Cl ratios in EGM from roof and floor cumulates vary largely in a similar range (0.001 to 0.05×10^{-3}). In the evolved rocks I/Cl ratios in EGM are comparatively high and less variable (0.01 to 0.05×10^{-3}) but are still overlapping (Figure 5). No easily recognizable trends are obvious, but part of these variations can be explained due to lower Cl concentrations in lujavrite samples. Still, as the Cl contents in the lujavrites are only about 2 to 3 times lower than in the roof and floor cumulates and the median I/Cl ratios of the lujavrite samples are about 4 times higher than those in the roof and floor cumulates, I enrichment in the lujavrite samples is suggested. Nevertheless, further research with methods more sensitive to I in EGM are necessary to better understand these observations.
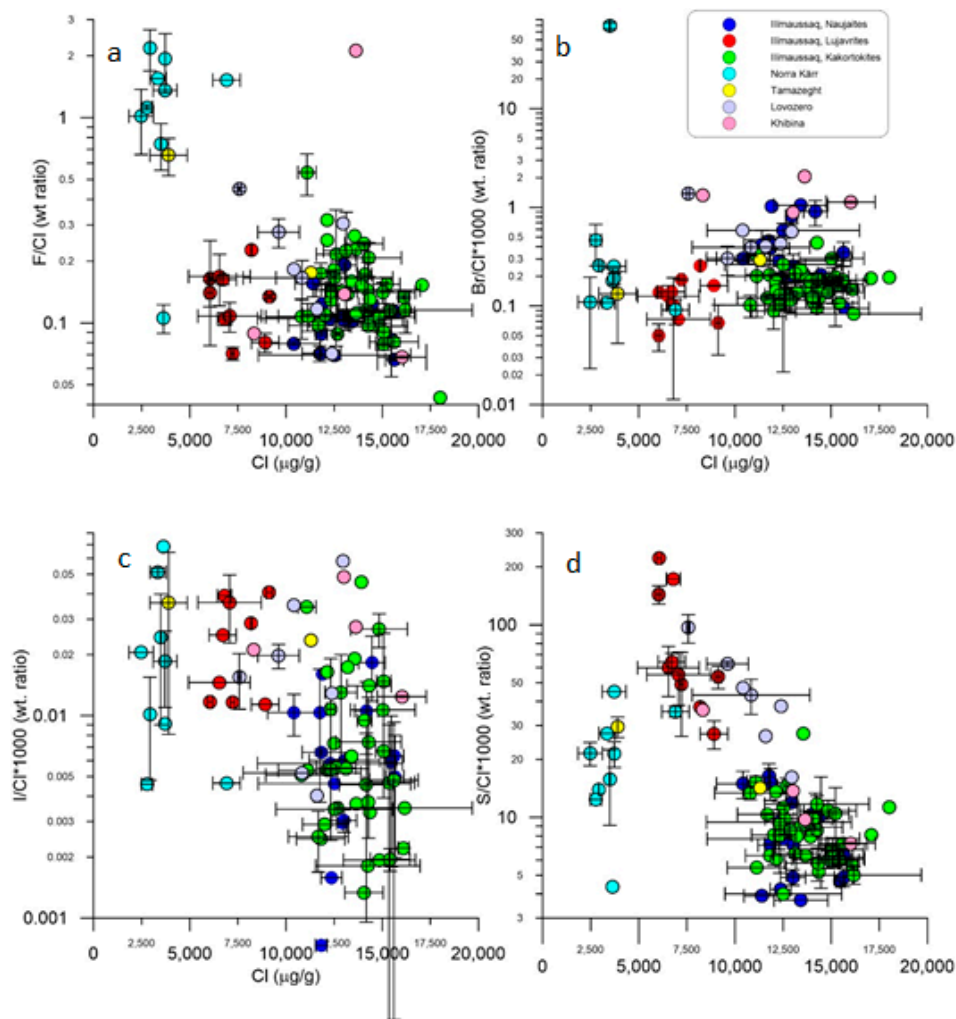
Figure 5. X/Cl versus Cl systematics in EGM. (**a**) Relationship between F/Cl and Cl. (**b**) Relationship between Br/Cl × 1000 and Cl. (**c**) Relationship between I/Cl × 1000 and Cl. (**d**) Relationship between S/Cl × 1000 and Cl.

The S/Cl ratios in EGM from roof and floor cumulates are below 0.03 and are largely overlapping, but EGM from lujavrites are comparatively S-rich with S/Cl values up to about 0.2 (Figure 5). The high S contents and S/Cl ratios in EGM from the evolved rocks are not analytical artefacts because (i) other S-bearing minerals in lujavrites are very rare [98], (ii) the samples with the highest S and S/Cl rations (Figures 3 and 5) represent some of the most evolved lujavrites of the section and whole-rock S contents for these rocks (up to 0.15 wt.% S) are much higher than for the other Ilímaussaq rocks (up to 0.08 wt.% S [40]) and (iii) previous microprobe data also indicate high S contents in sodalite from lujavrite rocks [63]. The roughly negative relationship between the Cl content and the S/Cl ratio in EGM (Figure 5) may indicate that while the Cl contents in EGM decreases due to lower Cl contents in the residual melt, S in this melt is passively enriched and incorporated in EGM. Alternatively, S incorporation in EGM from lujavrites is enhanced because of changing redox conditions (see below).

5.1.2. Sodalite

Figure 6 shows the anion vs. Cl trends for the sodalite (and tugtupite) samples. We use this way of plotting the data as the observed Cl concentration varies strongly. This probably is the due to the effect of inclusion of accessory minerals in the samples used in ion chromatography. The Br/Cl ratios in magmatic sodalite systematically decrease downwards the roof sequence from about 1.5×10^{-3} to values below 0.5×10^{-3}, a trend that is rather similar to the trend observed for EGM (compare also

Figures 3 and 4; see above). Br/Cl ratios in the few sodalite samples from floor cumulates are close to the lowest roof cumulate concentrations that were observed (around 0.5×10^{-3}). As sodalite in the roof cumulates is an early magmatic mineral (while EGM crystallized later), this suggests that the Br content in the melt decreases strongly by incorporation in sodalite. In contrast, I/Cl ratios in sodalite from roof cumulates are mostly lower than those from floor cumulates (Figure 6). No obvious trend indicating enrichment or depletion of I during magmatic evolution in the roof cumulates is observed, although the higher ratios in the interstitial sodalite in the floor cumulates may indicate concentration of I in the final stage of the melt.
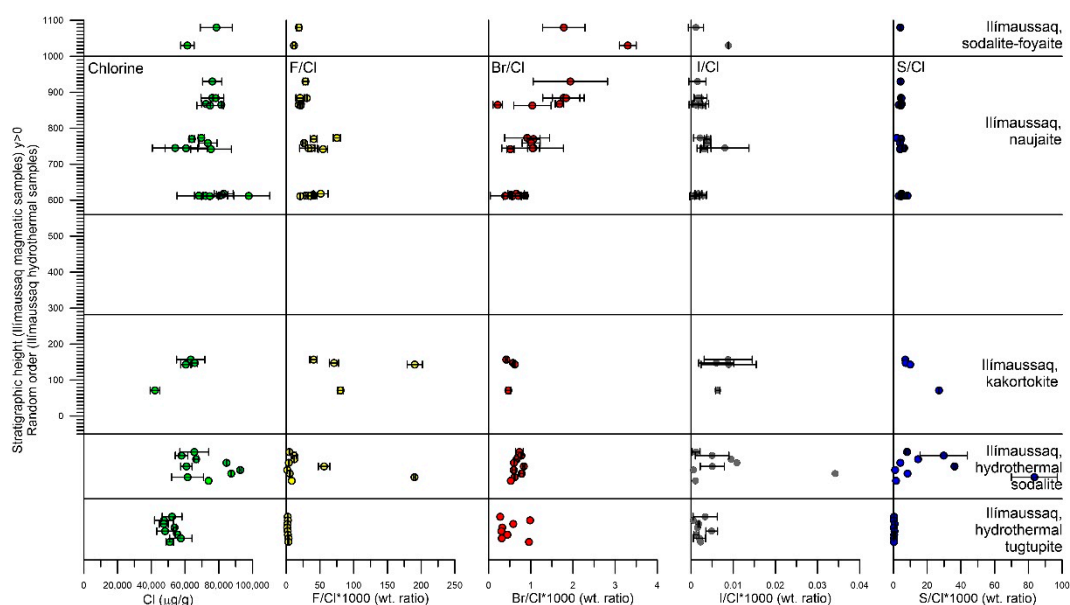
Figure 6. X/Cl and Cl systematics in sodalite and tugtupite. Cl concentration data are the same as in Figure 4 and are added for easy comparison between the Cl contents and the X/Cl ratios in the sodalite samples. Although tugtupite data are not discussed in the text (other than in the results section) they are incorporated for completeness and easy comparison to the concentration data in Figure 4. Magmatic Ilímaussaq samples are sorted according to their stratigraphic height in the intrusion, other samples are randomly ordered within each group.

Br/Cl ratios in fluid inclusions from late-stage quartz and fluorite are comparatively high, reaching values of around 9×10^{-3} [99] and suggest preferential loss of Br relative to Cl during fluid exsolution. Although hydrothermal sodalite may have formed from such Br-rich fluids, their Br/Cl ratios overlap with those of the magmatic sodalites from roof and floor cumulates.

Magmatic sodalite has in general significantly higher F/Cl ratios ($10–50 \times 10^{-3}$) than hydrothermal sodalite ($1–12 \times 10^{-3}$, Figure 4) and significantly lower F/Cl ratios than EGM. For that reason, F/Cl ratios of sodalite are plotted like the other anion/Cl ratios (thus $\times 10^{-3}$) for clarity. These data suggest limited capacity for incorporation of F during hydrothermal conditions. Interestingly the low F/Cl hydrothermal sodalite samples have in general relatively high (but very variable) S/Cl ratios. In the roof cumulates, F/Cl ratios are variable, but maximum ratios gradually decrease from base to top, suggesting that incorporation of F in sodalite slightly increases during the cooling of the melt. This also explains why F/Cl ratios are highest in the interstitial sodalite of the floor cumulates. The highest F/Cl ratio of 190×10^{-3} may however be explained by contamination with a F-rich mineral. Very low F/Cl ratios in hydrothermal sodalite can be explained by different exchange reactions and/or because most F is incorporated in specific F minerals such as fluorite and villiaumite and not as accessory ion in sodalite.

Low S/Cl ratios in magmatic sodalite from floor and roof cumulates (see above) are in accordance with previous data [54,63,100]. Unfortunately, we were unable to analyze sodalite from lujavrite rocks

but Markl et al. [63] report up to 1.5 wt.% S (based on EPMA, equivalent to an S/Cl ratio of 274×10^{-3}) for sodalites from these evolved rocks, which is much higher and in accordance with relatively high S contents in EGM from lujavrites (see above). We also observe higher S/Cl ratios in sodalite from the floor cumulates than in roof cumulates. The S/Cl variability in the hydrothermal sodalite samples is particularly large, showing both some of the lowest and some of the highest ratios observed (Figure 6). These differences can possibly be related to enrichment of S in the residual Ilímaussaq magmas/fluids (for samples with S enrichment) or to changes in redox conditions/water activity (that may also lead to depreciation of S). The most common S-species in natural SGMs (sodalite group minerals) are sulfate (SO_4^{2-}) and sulfide (S^{2-}), which can, depending on redox conditions, continuously substitute for each other [100–103]. Ilímaussaq sodalites are among the most reduced sodalites known (ΔFMQ-values below -1 [100]) and as a result their S consists mostly (or uniquely) of sulfide. Markl et al. [63] suggest that the late state melt from which lujavrites crystallize have more oxidising characteristics (ΔFMQ-values above $+2$) at which values it is expected that S is present mostly as sulfate ions. The data thus suggest that S in roof and floor cumulates (with low S contents) is mostly reduced sulfide, while S in lujavrite and some of the hydrothermal sodalites (with high S contents) is mostly oxidized sulfate.

5.2. Halogen and S Partitioning Between EGM and Sodalite

Rock samples from which sufficient EGM and sodalite for CIC analysis could be extracted enable us to investigate the partitioning of halogens and S between the two minerals (Figure 7). Importantly, the textural relationships and modal amounts of EGM and sodalite are different in the two rock types. Roof cumulates (naujaites) contain euhedral sodalite with moderate amounts of interstitial EGM, whereas in floor cumulates (kakortokites), EGM always largely dominates over sodalite and the latter is interstitial towards EGM.

Fluorine is clearly concentrated in EGM over sodalite, with relative enrichment factors ($[F/Cl_{EGM}/F/Cl_{sod})]$) between 2 and 6, averaging around 3 (Figure 7a). The relative enrichment in EGM compared to sodalite is related to the crystal structures of the two minerals. In sodalite each Cl is tetrahedrally surrounded by sodium with Na-Cl distances of 274 pm [104]. These authors also calculated the Na-F distance of the not yet synthesized F-sodalite, which is 228.3 pm, significantly smaller than the distance in Cl-sodalite. As the sodalite structure is relatively rigid, based on a cubic ordered framework of AlO_4 and SiO_4 tetrahedra the small F ion does not fit properly into the Cl space and it will prefer to stay in solution relative to Cl during sodalite crystallisation, or, if F-sodalite was a stable mineral and the F concentration was high enough, it would form F-sodalite. In EGM, Na is also only bonded to Cl. In EGM the chemical structure is much less constant as in sodalite and bond lengths seem to be more variable [105–107]. Johnsen and Grice [107] present the crystal structures of 17 different EGM crystals where F/Cl ratios vary between 0 and 5.7. Interatomic distances are given in detail for three of these crystals with F/Cl ratios of 0, 0.55, and 5.7. Na-X distances are variable, but largely overlapping with values between 236 and 283 pm overall with averages of 258 pm for the F-poorest crystal and 268 and 269 for the F-rich crystals. What we notice here is that average bond lengths for Cl-rich and F-rich EGM are very similar, suggesting that F can be incorporated as good as Cl. This suggests that F will preferably be incorporated in EGM compared to sodalite, because it fits better.

Bromine is mostly concentrated in sodalite relative to EGM (Figure 7b) except for one sample, with relative enrichment factors ($[Br/Cl_{EGM}/Br/Cl_{sod}]$) of about 0.5. The bond length for Na-Br in Br-sodalite is 286.5 pm [104]. Unfortunately, Na-Br bond lengths for EGM are not known. In the case of Br-sodalite the bond length is only moderately larger than the 274 pm for the Na-Cl bond length (ca. 5%). Br would fit fairly easy in a Cl-sodalite crystal. Considering that F and Cl fit equally easy in an EGM crystal could suggest that Br would also fit well in EGM. As the Br ion seems to prefer sodalite over EGM, this would suggest the Br prefers the crystal where it fits in a fixed Na-tetrahedron compared to a crystal where it is rather loosely bound to the Na ions in its surroundings. As no quantitative data for Br in EGM are known, further research is necessary to better understand its behavior in EGM.

Although I concentrations are very low in the samples, I/Cl enrichment factors ([I/Cl$_{EGM}$/I/Cl$_{sod}$)]) seem to indicate differences between samples from the roof and the floor cumulates (Figure 7c). In most roof cumulate samples, I concentrates in EGM, while in the floor cumulates it concentrates in the sodalite. I$^-$ is a very large ion (210 pm, compared to 167 pm for Cl$^-$ and 196 pm for Br$^-$ [25]) and does not fit well in most crystal structures. This suggests that it will only be incorporated in minerals in the last magmatic stages. Sodalites in the roof cumulates are early stage and EGM last stage minerals while in the floor cumulates EGM are more early stage and sodalite last. This fits relatively well, especially considering the very low I concentrations in these samples.
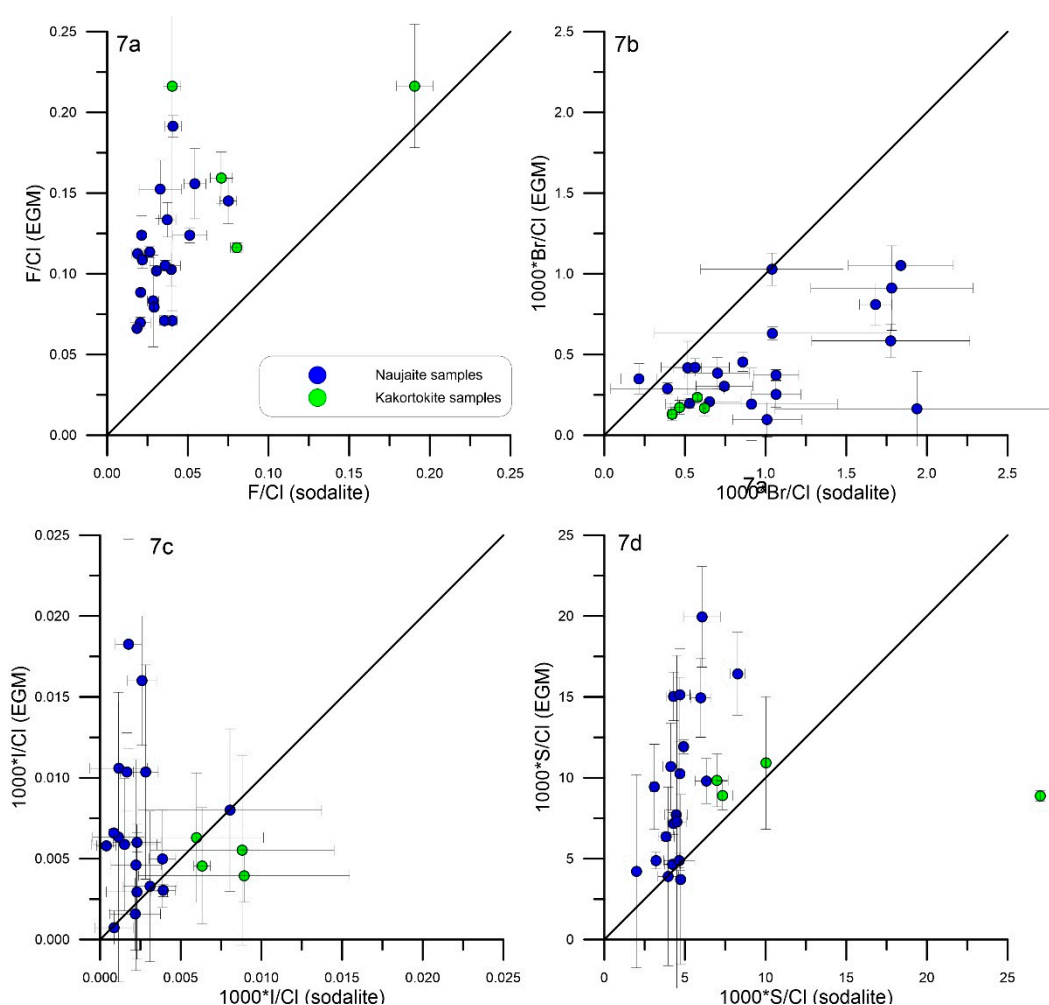
Figure 7. Comparison of (**a**) F/Cl, (**b**) Br/Cl, (**c**) I/Cl and (**d**) S/Cl, ratios between EGM and sodalite from the same rock samples. Sodalite seems to prefer Br compared to EGM, which relatively concentrates F and S. The preference I depends on rock type or crystallization conditions

The sulfur distribution between sodalite and EGM is similar to what was observed for F (except for one sample), showing preferred incorporation of S into EGM in most roof and some floor cumulate samples (Figure 7d) and suggesting that S fits more easily in EGM than in sodalite. A complicating factor here is the redox sensitivity of S. Following our discussion above (Section 5.1.2), S in magmatic sodalite from floor and roof series rocks in Ilímaussaq under reduced conditions is mostly present as S^{2-} and S tends to prefer EGM over sodalite. However, sodalite in evolved rocks that may have crystallized at higher water activity and oxygen fugacity is very S-rich [63] with S/Cl ratios (around 0.3) higher than in EGM (0.025–0.2). Assuming that S is present as sulfate in both minerals, under water-rich/more oxidized conditions, the compatibility of SO$_4^{2-}$ for sodalite is larger than for EGM.

5.3. Halogen and S Systematics of EGM from Different Localities: Clues to Magma Sources?

Between the five intrusive complexes (Ilímaussaq, Norra Kärr, Tamazeght, Lovozero, and Khibina) there is considerable variation both in F, Cl, Br, and S and in the Cl-normalized ratios (Figures 3 and 5). Very striking are the exceptionally high F and low Cl contents in EGM from Norra Kärr (Figures 3a and 5a). With generally around 0.4–0.7 wt.%, F in these EGM is mostly even higher than Cl (0.3–0.4 wt%), which indicates that on a molar basis, F is about twice as high as Cl). At the other locations (Tamazeght, Lovozero, and Khibina), F/Cl ratios are much more in line with the ratios observed in Ilímaussaq. The data clearly show that F is always a very common minor component in EGM with concentrations of around 0.1–0.3 wt.% (Figure 3). Molar F/Cl ratios of EGM from Norra Kärr can be higher than 1, whereas those from Tamazeght, Lovozero, and Khibina are mostly similar to Ilímaussaq samples and generally well below 0.5 (Figure 5b). In contrast to the other studied complexes, Norra Kärr is characterized by the total absence of sodalite and is relatively poor in typical F-carriers in such systems, such as fluorite and sodic amphibole [58,78]. This may indicate a relatively Cl-poor parental magma compared to the other studied complexes, or it may indicate that halogens were lost during metamorphism. The first explanation would result in a system in which F needed to be incorporated in EGM and could explain the exceptionally high F/Cl ratios in EGM. Unlike the other intrusions, Norra Kärr has been deformed and metamorphosed and shows intense interaction with crustal fluids. Atanasova et al. [58] state that EGM were formed once sufficient Cl (and REE and HFSE) were present. During metamorphism, EGM were destabilised and partly decomposed to catapleite ($Na_2Zr[Si_3O_9].2H_2O$) and secondary REE bearing minerals. As the high F contents of EGM in Norra Kärr were not realised at that time (no F data were reported in [58]) it is not possible to establish the importance of the presence of F in this system yet. It must be realized, however, that it is also unknown yet if Cl is an essential element in the formation of EGM. Although a F-bearing endmember (kentbrooksite [106]) has been defined already more than 20 years ago, the importance of F in EGM has not been realised yet. Giehl et al. [16] in their study on the experimental evolution of peralkaline melts were not able to measure F in EGM that were formed during their experiments and for that reason it is impossible to understand F-Cl relationships during formation of EGM from melts that contain significant F and Cl amounts. F is only very seldomly measured in EGM, as its detection limit at the EPMA is rather high and it cannot be measured by ICP-MS. As a result, this study is the first to obtain a rather comprehensive view of the presence of F in EGM.

Bromine contents and Br/Cl ratios are highest in EGM from Khibina, in some samples even higher than in the roof cumulates from Ilímaussaq (Figures 2 and 5). As progressive crystallization of sodalite and EGM decreases Br/Cl ratios (see above), this suggests that Khibina represents a relatively "less-evolved" magma composition compared to the closely associated Lovozero complex, which is often considered as closely related to the Khibina complex [52,73]. The Br/Cl ratio content in Lovozero is comparable to the naujaite samples from Ilímaussaq, and higher than in the kakortokites. The Br/Cl ratios in EGM from Tamazeght are more in line with the kakortokites. Br/Cl ratios in Norra Kärr are mostly in line with the ratios in Ilímaussaq. The low Cl in this location indicates that Br is also mostly low. In one sample, however, an extremely high Br concentration was observed. In sample NK5613 a concentration of 480 µg/g was measured. While extreme, as otherwise no concentrations in EGM above 28 were measured, the value is real; although at first it was thought that the sample was contaminated. A recent study [108] measured Br concentrations in a small number of Norra Kärr EGM by LA-ICP-MS. They measured in each of their three samples Br concentrations that were mostly above 100 µg/g. That indicates that Br in EGM can in principle be very high. As the EGM in Norra Kärr are metamorphosed and altered it may be possible that parts of them have been heavily altered by very Br rich aqueous solution resulting in extreme Br incorporation in parts of the EGM here.

Sulfur concentrations are relatively high in samples from Lovozero. Both absolute S concentrations and S/Cl ratios are comparable to the contents of the "lower S" Lujavrites from Ilímaussaq, but significantly lower than the very high S contents in the top lujavrites. S contents in the other complexes are comparable to the contents in the top and floor cumulates from Ilímaussaq.

The variability of the minor anion (F-Br-S) geochemistry of EGM in different peralkaline complexes is well illustrated in a ternary F-S-100 × Br diagram (Figure 8). It shows very nicely that the minor anion chemistry of EGM varies greatly from location to location. It also shows that there are no fixed relationships between the minor anions and that their relationships are affected by chemical variations in the melt and by post-magmatic processes. The ternary diagram illustrates the F-rich nature of EGM from Norra Kärr, the relatively high Br contents for EGM from Khibina and from Ilímaussaq naujaites, the relatively S-rich nature of EGM from Ilímaussaq lujavrites and intermediate positions for EGM from Lovozero (Figure 8).
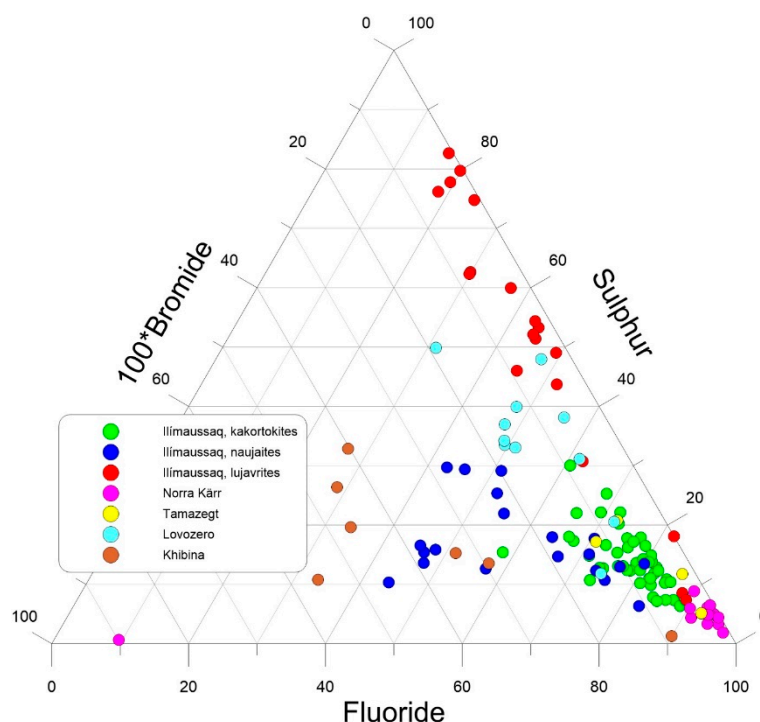
Figure 8. Ternary F-S-Br for EGM from five peralkaline intrusions illustrating clear differences in halogen and sulfur systematics.

6. Conclusions

Halogen systematics and halogen ratios in Cl-dominated rock-forming minerals in peralkaline rocks monitor magmatic processes (e.g., fractionation and cumulate formation) and late-stage hydrothermal processes (degassing, water-enrichment, and fluid–rock interaction).

We have determined the halogen (F, Cl, Br, and I) and S contents in a set of eudialyte-group minerals, sodalites and tugtupites from five different peralkaline intrusions (Ilímaussaq, Norra Kärr, Tamazeght, Lovozero, and Khibina), with a clear focus on EGM and sodalite samples from the well-studied Ilimaussaq complex. The detailed knowledge for these samples allows to correlate changes in halogen contents and ratios with processes, based on numerous previous studies on these rocks. The investigated minerals dominate the Cl and Br budget of the rocks, while for F, other F-bearing phases (e.g., amphibole, fluorite, villiaumite, and minerals of the rinkite group and the apatite supergroup) play a role in some of the investigated rocks. Parts of the S budget are scavenged in rare sulfides.

On an intrusion scale, fractionation of sodalite and EGM in peralkaline magmas leads to decreasing Cl and Br contents as well as Br/Cl ratios in the system during magmatic evolution. This parallels apatite fractionation in metaluminous rocks, causing decreasing Br/Cl in evolved rocks, with generally decreasing Br and Cl contents, while F increases [9]. Fluorine contents in sodalite and EGM are, however, difficult to interpret in the case of peralkaline systems as several other F-rich phases

contribute to the F budget of the magma. Because of its redox sensitivity, S contents in sodalite and EGM show the combined effects of magma differentiation and changes in oxygen fugacity and water activity. Low I contents render it not easy to constrain the behavior of this rare and barely studied element during magmatic differentiation and hydrothermal overprint. Although there are responses to changing physico-chemical crystallization conditions, it remains difficult to draw more quantitative conclusions. Understanding I better in evolving magmatic systems requires application of more sensitive methods than the CIC setting applied here (e.g., SIMS techniques) using carefully characterized and matrix-matched reference materials.

Our data also bear implications for the mineral chemistry and compositional variation of sodalite and especially EGM in general. Volatile components in EGM that are not normally considered, such as F and S, can reach concentrations of thousands of μg/g. Especially in the case of F, with its low atomic weight, the results obtained in this study indicate that it is very significant for formulae calculations, neutral charge-balance, and similar aspects at such concentration levels. Further dedicated research on the distribution of minor anions (F, Br, S, and I) is extremely sparse and clearly needed for a full understanding on the impact of these components on the crystallography and structure refinement methods for this mineral group.

References

1. Aiuppa, A.; Baker, D.R.; Webster, J.D. Halogens in volcanic systems. *Chem. Geol.* **2009**, *263*, 1–18. [CrossRef]
2. Pyle, D.M.; Mather, T.A. Halogens in igneous processes and their fluxes to the atmosphere and oceans from volcanic activity: A review. *Chem. Geol.* **2009**, *263*, 110–121. [CrossRef]
3. Gerlach, T.M. Volcanic sources of tropospheric ozone-depleting trace gases. *Geochem. Geophys. Geosyst.* **2004**, *5*, 16. [CrossRef]
4. Oppenheimer, C.; Bani, P.; Calkins, J.A.; Burton, M.R.; Sawyer, G.M. Rapid FTIR sensing of volcanic gases released by strombolian explosions at Yasur volcano, Vanuatu. *Appl. Phys. B* **2006**, *85*, 453–460. [CrossRef]
5. Theys, N.; Van Rozendael, M.; Dils, B.; Hendrick, F.; de Mazière, M. First satellite detection of volcanic bromine monoxide emission after Kasatochi eruption. *Geophys. Res. Lett.* **2009**, *36*, L03809. [CrossRef]
6. Daniel, J.S.; Solomon, S.; Portmann, R.W.; Garcia, R.R. Stratospheric ozone detruction: The importance of bromine relative to chlorine. *J. Geophys. Res.* **1999**, *104*, 23871–23880. [CrossRef]
7. Bureau, H.; Foy, E.; Raepsaet, C.; Somogyi, A.; Munsch, P.; Simon, G.; Kubsky, S. Bromine cycle in subduction zones through in situ Br monitoring in diamond anvil cells. *Geochim. Cosmochim. Acta* **2010**, *74*, 3839–3850. [CrossRef]
8. Boulyga, S.F.; Heumann, K.G. Direct determination of halogens in powdered geological and environmental samples using isotope dilution laser ablation ICP-MS. *Int. J. Mass Spectrom.* **2005**, *242*, 291–296. [CrossRef]

9. Marks, M.A.W.; Wenzel, T.; Whitehouse, M.; Loose, M.; Zack, T.; Barth, M.; Worgard, L.; Krasz, V.; Eby, G.N.; Stosnach, H.; et al. The volatile inventory (F, Cl, Br, S, C) of magmatic apatite: An integrated analytical approach. *Chem. Geol.* **2012**, *291*, 241–255. [CrossRef]

10. John, T.; Scambelluri, T.; Frische, M.; Barnes, J.D.; Bach, W. Dehydration of subducting serpentinite: Implications for halogen mobility in subduction zones and the deep halogen cycle. *Earth Planet. Sci. Lett.* **2011**, *308*, 65–76. [CrossRef]

11. Cadoux, A.; Iacono-Mariziano, G.; Paonita, A.; Deloule, E.; Aiuppa, A.; Eby, G.N.; Costa, M.; Brusca, L.; Berlo, K.; Geraki, K.; et al. A new set of standards for in–situ measurement of bromine abundances in natural silicate glasses: Application to SR-XRF, LA-ICP-MS and SIMS techniques. *Chem. Geol.* **2017**, *452*, 60–70. [CrossRef]

12. Zhang, C.; Lin, J.; Pan, Y.; Feng, R.; Almeev, R.R.; Holtz, F. Electron Probe Microanalysis of Bromine in Minerals and Glasses with Correction for Spectral Interference from Aluminium, and Comparison with Microbeam Synchrotron X-Ray Fluorescence Spectrometry. *Geostand. Geoanal. Res.* **2017**, *41*, 449–457. [CrossRef]

13. Webster, J.D. Partitioning of F between H_2O and CO_2 fluids and topaz rhyolite melt. *Contrib. Mineral. Petrol.* **1990**, *104*, 424–438. [CrossRef]

14. Webster, J.D.; Halloway, J.R. Partitioning of F and Cl between magmatic hydrothermal fluids and highly evolved granitic magmas. *Geol. Soc. Am. Spec. Pap.* **1990**, *246*, 21–34.

15. Scaillet, B.; Macdonald, R. Fluorite stability in silicic magmas. *Contrib. Mineral. Petrol.* **2004**, *147*, 319–329. [CrossRef]

16. Giehl, C.; Marks, M.A.W.; Nowak, M. An experimental study on the influence of fluorine and chlorine on phase relations in peralkaline phonolitic melts. *Contrib. Mineral. Petrol.* **2014**, *167*, 977. [CrossRef]

17. Metrich, N.; Rutherford, M.J. Experimental study of chlorine behaviour in hydrous silicic melts. *Geochim. Cosmochim. Acta* **1992**, *56*, 607–616. [CrossRef]

18. Signorelli, S.; Carroll, M.R. Solubility and fluid-melt partitioning of Cl in hydrous phonolitic melts. *Geochim. Cosmochim. Acta* **2000**, *64*, 2851–2862. [CrossRef]

19. Signorelli, S.; Carroll, M.R. Experimental study of Cl solubility in hydrous alkaline melts: Constraints on the theoretical maximum amount of Cl in trachytic and phonolitic melts. *Contrib. Mineral. Petrol.* **2002**, *143*, 209–218.

20. Bureau, H.; Métrich, N. An experimental study of bromine behaviour in water-saturated silicic melts. *Geochim. Cosmochim. Acta* **2003**, *67*, 1689–1697. [CrossRef]

21. Bureau, H.; Keppler, H.; Métrich, N. Volcanic degassing of bromine and iodine: Experimental fluid/melt partitioning data and applications to stratospheric chemistry. *Earth Planet. Sci. Lett.* **2000**, *183*, 51–60. [CrossRef]

22. Carroll, M.R.; Webster, J.D. Solubilities of sulfur, noble gases, nitrogen, chlorine and fluorine in magmas. *Rev. Miner.* **1994**, *30*, 231–279.

23. Villemant, B.; Boudon, G. H_2O and halogen (F, Cl, Br) behaviour during shallow agma degassing processes. *Earth Planet. Sci. Lett.* **1999**, *168*, 271–286. [CrossRef]

24. Wang, L.-X.; Marks, M.A.W.; Keller, J.; Markl, G. Halogen variations in alkaline rocks from the Upper Rhine Graben (SW Germany): Insights into F, Cl and Br behavior during magmatic processes. *Chem. Geol.* **2014**, *380*, 133–144. [CrossRef]

25. Shannon, R.D. Revised effective ionic radii and systematic studies of interatomic distances in halides and chalcogenides. *Acta Crystallogr. A* **1976**, *32*, 751–767. [CrossRef]

26. Dong, P. Halogen-Element (F, Cl and Br) Behaviour in Apatites, Scapolite, and Sodalite: An Experimental Investigation with Field Applications. Ph.D. Thesis, University of Saskatchewan, Saskatoon, SK, Canada, 2005.

27. Piccoli, P.M.; Candela, P.A. Apatite in igneous systems. *Rev. Mineral. Geochem.* **2002**, *48*, 255–292. [CrossRef]

28. Zhang, C.; Holtz, F.; Ma, C.; Wolff, P.E.; Li, X. Tracing the evolution and distribution of F and Cl in plutonic systems from volatile-bearing minerals: A case study from the Liujiawa pluton (Dabie Orogen, China). *Contrib. Mineral. Petrol.* **2012**, *164*, 859–879. [CrossRef]

29. Teiber, H.; Marks, M.A.W.; Wenzel, T.; Zack, T.; Siebel, W.; Altherr, R.; Markl, G. The distribution of halogens (F, Cl, Br) in granitoid rocks. *Chem. Geol.* **2014**, *374–375*, 92–109. [CrossRef]

30. Zhu, C.; Sverjenski, D.A. Partitioning of F-Cl-OH between minerals and hydrothermal fluids. *Geochim. Cosmochim. Acta* **1991**, *55*, 1837–1858. [CrossRef]

31. Ionov, D.A.; Griffin, W.L.; O'Reilly, S.Y. Volatile-bearing minerals and lithophile trace elements in the upper mantle. *Chem. Geol.* **1997**, *141*, 153–184. [CrossRef]

32. Kendrick, M.A. High precision Cl, Br and I determinations in mineral standards using the noble gas method. *Chem. Geol.* **2012**, *292*, 116–126. [CrossRef]

33. Krumrei, T.V.; Pernicka, E.; Kaliwoda, M.; Markl, G. Volatiles in a peralkaline system: Abiogenic hydrocarbons and F-Cl-Br systematics in the naujaite of the Ilimaussaq intrusion, South Greenland. *Lithos* **2007**, *95*, 298–314. [CrossRef]

34. O´Reilly, S.Y.; Griffin, W.L. Apatite in the mantle: Implications for metasomatic processes and high heat production in Phanerozoic mantle. *Lithos* **2000**, *53*, 217–232. [CrossRef]

35. Kusebauch, C.; John, T.; Whitehouse, M.J.; Engvik, A.K. Apatite as probe for the halogen composition of metamorphic fluids (Bamble Sector, SE Norway). *Contrib. Mineral. Petrol.* **2015**, *170*, 34. [CrossRef]

36. Kusebauch, C.; John, T.; Barnes, J.D.; Klügel, A.; Austrheim, H.O. Halogen Element and Stable Chlorine Isotope Fractionation Caused by Fluid–Rock Interaction (Bamble Sector, SE Norway). *J. Petrol.* **2015**, *56*, 299–324. [CrossRef]

37. Teiber, H.; Marks, M.A.W.; Arzamastsev, A.A.; Wenzel, T.; Markl, G. Compositional variation in apatite from various host rocks: Clues with regards to source composition and crystallization conditions. *Neues Jahrb. Mineral. Abh. J. Mineral. Geochem.* **2015**, *192*, 151–167. [CrossRef]

38. Wang, L.-X.; Marks, M.A.W.; Wenzel, T.; von der Handt, A.; Keller, J.; Teiber, H.; Markl, G. Apatites from the Kaiserstuhl Volcanic Complex, Germany: New constraints on the relationship between carbonatite and associated silicate rocks. *Eur. J. Mineral.* **2014**, *26*, 397–414. [CrossRef]

39. Wang, L.-X.; Marks, M.A.W.; Wenzel, T.; Markl, G. Halogen-bearing minerals from the Tamazeght complex (Morocco): Constraints on halogen distribution and evolution in alkaline to peralkaline magmatic systems. *Can. Mineral.* **2016**, *54*, 1347–1368. [CrossRef]

40. Bailey, J.C.; Gwozdz, R.; Rose-Hansen, J.; Sørensen, H. Geochemical overview of the Ilimaussaq alkaline complex, South Greenland. *GEUS Bull.* **2001**, *190*, 35–53. [CrossRef]

41. Smith, M.; Moore, K.; Kavecsánszki, D.; Finch, A.; Kynicky, J.; Wall, F. From mantle to critical zone: A review of large and giant sized deposits of the rare earth elements. *Geosci. Front.* **2016**, *7*, 315–334. [CrossRef]

42. Goodenough, K.M.; Schilling, J.; Jonsson, E.; Kalvig, P.; Charles, N.; Tuduri, J.; Deady, E.A.; Sadeghi, M.; Schiellerup, H.; Müller, A.; et al. Europe's rare earth element resource potential: An overview of REE metallogenetic provinces and their geodynamic setting. *Ore Geol. Rev.* **2016**, *72*, 838–856. [CrossRef]

43. Khomyakov, A. *Mineralogy of Hyperagpaitic Alkaline Rocks*; Oxford Science Publications; Oxford University Press: Oxford, UK, 1995; 222p.

44. Sørensen, H. The agpaitic rocks—An overview. *Mineral. Mag.* **1997**, *61*, 485–498. [CrossRef]

45. Andersen, T.; Erambert, M.; Larsen, A.O.; Selbekk, R.S. Petrology of nepheline syenite pegmatites in the Oslo rift, Norway: Zirconium silicate mineral assemblages as indicators of alkalinity and volatile fugacity in mildly agpaitic magma. *J. Petrol.* **2010**, *51*, 2303–2325. [CrossRef]

46. Marks, M.A.W.; Hettmann, K.; Schilling, J.; Frost, B.R.; Markl, G. The mineralogical diversity of alkaline igneous rocks: Critical factors for the transition from miaskitic to agpaitic phase assemblages. *J. Petrol.* **2010**, *52*, 439–455. [CrossRef]

47. Marks, M.A.W.; Markl, G. A global review on agpaitic rocks. *Earth Sci. Rev.* **2017**, *173*, 229–258. [CrossRef]

48. Lindhuber, M.J.; Marks, M.A.W.; Bons, P.D.; Wenzel, T.; Markl, G. Crystal mat-formation as an igneous layering-forming process: Textural and geochemical evidence from the 'lower layered' nepheline syenite sequence of the Ilimaussaq complex, South Greenland. *Lithos* **2015**, *224–225*, 295–309. [CrossRef]

49. Ratschbacher, B.C.; Marks, M.A.W.; Bons, P.D.; Wenzel, T.; Markl, G. Emplacement and geochemical evolution of highly evolved syenites investigated by a combined structural and geochemical field study: The lujavrites of the Ilímaussaq complex, SW Greenland. *Lithos* **2015**, *231*, 62–76. [CrossRef]

50. Stormer, J.C.; Carmichael, I. Villiaumite and the occurrence of fluoride minerals in igneous rocks. *Am. Mineral.* **1970**, *55*, 126–134.

51. Sharp, Z.D.; Helffrich, G.R.; Bohlen, S.R.; Essene, E.J. The stability of sodalite in the system $NaAlSiO_4$-$NaCl$. *Geochim. Cosmochim. Acta* **1989**, *53*, 1943–1954. [CrossRef]

52. Kogarko, L.N.; Lazutkina, L.N.; Romanchev, B.P. The origin of eudialyte mineralization (translated from Russian). *Geokhimiya* **1982**, *10*, 1415–1432.

53. Bailey, J.C. Geochemistry of boron in the Ilimaussaq alkaline complex, South Greenland. *Lithos* **2006**, *91*, 319–330. [CrossRef]

54. Zahoransky, T.; Friis, H.; Marks, M.A.W. Luminescence and tenebrescence of natural sodalites: A chemical and structural study. *Phys. Chem. Mineral.* **2016**, *43*, 459–480. [CrossRef]

55. Pan, Y.; Dong, P. Bromine in scapolite-group minerals and sodalite; XRF microprobe analysis, exchange experiments, and applications to skarn deposits. *Can. Mineral.* **2003**, *41*, 529–540. [CrossRef]

56. Ryabchikov, I.D.; Kogarko, L.N. Oxygen fugacity in the apatite-bearing intrusion of the Khibina complex. *Geochem. Int.* **2009**, *47*, 1157–1169. [CrossRef]

57. Arzamastsev, A.A.; Glaznev, V.N.; Raevsky, A.B.; Arzamastseva, L.V. Morphology and internal structure of the Kola Alkaline intrusions, NE Fennoscandian Shield: 3D density modelling and geological implications. *J. Asian Earth Sci.* **2001**, *18*, 213–228. [CrossRef]

58. Atanasova, P.; Marks, M.A.W.; Heining, T.; Krause, J.; Gutzmer, J.; Markl, G. Distinguishing magmatic and metamorphic processes in peralkaline rocks of the Norra Kärr complex (Southern Sweden) using textural and compositional variations of clinopyroxene and eudialyte-group minerals. *J. Petrol.* **2017**, *58*, 361–384. [CrossRef]

59. Kramm, U.; Kogarko, L.N. Nd and Sr isotope signatures of the Khibina and Lovozero agpaitic centres, Kola Alkaline province, Russia. *Lithos* **1994**, *32*, 225–242. [CrossRef]

60. Schilling, J.; Wu, F.-Y.; McCammon, C.; Wenzel, T.; Marks, M.A.W.; Pfaff, K.; Jacob, D.E.; Markl, G. The compositional variability of eudialyte-group minerals. *Mineral. Mag.* **2011**, *75*, 87–115. [CrossRef]

61. Marks, M.A.W.; Markl, G. The Ilímaussaq alkaline complex, South Greenland. In *Layered Intrusions*; Charlier, B., Namur, O., Latypov, R., Tegner, C., Eds.; Springer Geology; Springer: Dordrecht, The Netherlands, 2015; pp. 649–691.

62. Larsen, L.M.; Sørensen, H. The Ilimaussaq intrusion-progressive crystallization and formation of layering in an agpaitic magma. In *Alkaline Igneous Rocks*; Fitton, J.G., Upton, B.G.J., Eds.; Geological Society Special Publications; Blackwell Scientific Publications: London, UK, 1987; Volume 30, pp. 473–488.

63. Markl, G.; Marks, M.; Schwinn, G.; Sommer, H. Phase equilibrium constraints on intensive crystallization parameters of the Ilimaussaq Complex, South Greenland. *J. Petrol.* **2001**, *42*, 2231–2258. [CrossRef]

64. Marks, M.A.W.; Rudnick, R.; Vennemann, T.; McCammon, C.; Markl, G. Arrested kinetic Li isotope fractionation at the margin of the Ilimaussaq complex, South Greenland: Evidence for open-system processes during final cooling of peralkaline igneous rocks. *Chem. Geol.* **2007**, *246*, 207–230. [CrossRef]

65. Schönberg, R.; Marks, M.A.W.; Schuessler, J.A.; von Blanckenburg, F.; Markl, G. Fe isotope systematics of coexisting amphibole and pyroxene in the alkaline igneous rock suite of the Ilímaussaq Complex, South Greenland. *Chem. Geol.* **2009**, *258*, 65–77. [CrossRef]

66. Hettmann, K.; Marks, M.A.W.; Kreissig, K.; Zack, T.; Wenzel, T.; Rehkämper, M.; Jacob, D.E.; Markl, G. The geochemistry of Tl and its isotopes during magmatic and hydrothermal processes: The peralkaline Ilimaussaq complex, southwest Greenland. *Chem. Geol.* **2014**, *366*, 1–13. [CrossRef]

67. Kchit, A. Le Plutonisme Alcalin du Tamazeght (Haut Atlas de Midelt, Maroc). Ph.D. Thesis, University Toulouse, Toulouse, France, 1990; 224p.

68. Marks, M.A.W.; Schilling, J.; Coulson, I.M.; Wenzel, T.; Markl, G. The alkaline-peralkaline Tamazeght complex, High Atlas Mountains, Morocco: Mineral chemistry and petrological constraints for derivation from a compositionally heterogeneous mantle source. *J. Petrol.* **2008**, *49*, 1097–1131. [CrossRef]

69. Marks, M.; Coulson, I.M.; Schilling, J.; Jacob, D.E.; Schmitt, A.K.; Markl, G. The effect of titanite and other HFSE-rich mineral (Ti-bearing andradite, zircon, eudialyte) fractionation on the geochemical evolution of silicate melts. *Chem. Geol.* **2008**, *257*, 153–172. [CrossRef]

70. Marks, M.A.W.; Neukirchen, F.; Vennemann, T.; Markl, G. Textural, chemical, and isotopic effects of late-magmatic carbonatitic fluids in the carbonatite-syenite Tamazeght complex, High Atlas Mountains, Morocco. *Mineral. Petrol.* **2009**, *97*, 23–42. [CrossRef]

71. Allah, R.K.; Fontan, F.; Kadar, M.; Monchoux, P.; Sørensen, H. Reactions between agpaitic nepheline syenitic melts and sedimentary carbonate rocks, exemplified by the Tamazeght complex, Morocco. *Geochem. Int.* **1998**, *36*, 569–581.

72. Schilling, J.; Marks, M.; Wenzel, T.; Markl, G. Reconstruction of magmatic to sub-solidus processes in an agpaitic system using eudialyte textures and composition: A case study from Tamazeght, Morocco. *Can. Mineral.* **2009**, *47*, 351–365. [CrossRef]

73. Arzamastsev, A.A.; Yakovenchuk, V.; Pakhomovsky, Y.; Ivanyuk, G. The Khibina and Lovozero alkaline massifs: Geology and unique mineralization. In Proceedings of the 33 International Geological Congress (IGC) Excursion No 47, Oslo, Norway, 6–14 August 2008.

74. Zaitsev, A.N.; Wall, F.; Le Bas, M.J. REE-Sr-Ba minerals from the Khibina carbonatites, Kola Peninsula, Russia: Their mineralogy, paragenesis and evolution. *Mineral. Mag.* **1998**, *62*, 225–250. [CrossRef]

75. Arzamastsev, A.A.; Arzamastseva, L.V.; Zhirova, A.M.; Glaznev, V.N. Model of formation of the Khibiny-Lovozero ore-bearing volcanic-plutonic complex. *Geol. Ore Depos.* **2013**, *55*, 341–356. [CrossRef]

76. Mikhailova, J.A.; Ivanyuk, G.Y.; Kalashnikov, A.O.; Pakhomovsky, Y.A.; Bazai, A.V.; Yakovenchuk, V.N. Petrogenesis of the Eudialyte Complex of the Lovozero Alkaline Massif (Kola Peninsula, Russia). *Minerals* **2019**, *9*, 581. [CrossRef]

77. Ryabchikov, I.D.; Kogarko, L.N. Magnetite compositions and oxygen fugacity of the Khibina magmatic system. *Lithos* **2006**, *91*, 35–45. [CrossRef]

78. Sjöqvist, A.S.; Cornell, D.H.; Andersen, T.; Erambert, M.; Ek, M.; Leijd, M. Three Compositional Varieties of Rare-Earth Element Ore: Eudialyte-Group Minerals from the Norra Kärr Alkaline Complex, Southern Sweden. *Minerals* **2013**, *3*, 94–120. [CrossRef]

79. Stevensen, F.J. Chemical state of the nitrogen in rocks. *Geochim. Cosmochim. Acta* **1962**, *26*, 797–809. [CrossRef]

80. Scholten, S.O. The Distribution of Nitrogen Isotopes in Sediments. Ph.D. Thesis, Utrecht University Repository, Utrecht, The Netherlands, 1991.

81. Holloway, J.A.M.; Dahlgren, R.A. Nitrogen in rock: Occurrences and biogeochemical implications. *Glob. Biogeochem. Cycles* **2002**, *16*, 65. [CrossRef]

82. Walter, A. *Bestimmung von Iod in Gesteinsmehl nach Verbrennungsaufschluß mit Metrohm Combustion*; Application Work AW IC DE8-0898-042015; Metrohm: Filderstadt, Germany, 2016.

83. Hagen, M. Igneous Layering: Mineralogic and Petrologic Analysis of Slightly-Layered Kakortokites (SLK's) and Lower Layered Kakortokites (LLK's) of the Ilimaussaq Intrusion, Southwest Greenland. Master's Thesis, University of Tübingen, Tübingen, Germany, 2019.

84. Mundel, F. Igneous Layering in the Lowermost Units of the Eudialyte-Bearing Nepheline Syenitic Kakortokites, Ilímaussaq Alkaline Complex, South Greenland. Master's Thesis, Eberhard-Karls-Universität Tübingen, Tübingen, Germany, 2019.

85. Rastsvetaeva, R.K. Structural mineralogy of the eudialyte group: A review. *Crystallogr. Rep.* **2007**, *52*, 47–64. [CrossRef]

86. Rastsvetaeva, R.K.; Chukanov, N.V. Classification of eudialyte-group minerals. *Geol. Ore Depos.* **2012**, *54*, 487–497. [CrossRef]

87. Rastsvetaeva, R.K.; Chukanov, N.V.; Pekov, I.V.; Varlamov, D.A.; Aksenov, S.M. New Data on the Isomorphism in Eudialyte-Group Minerals. VI: Crystal Structure of the First Member Containing Sulfide Anion with Isomorphic Substitution Cl^--S^{2-}. *Crystallogr. Rep.* **2020**, *65*, 215–222. [CrossRef]

88. Sørensen, H.; Danø, M.; Petersen, O.V. On the mineralogy and paragenesis of Tugtupite, $Na_8Al_2Be_2Si_8O_{24}(Cl,S)_2$, from the Ilímaussaq alkaline intrusion, South Greenland. *GEUS Bull.* **1971**, *95*, 38.

89. Danø, M. The crystal structure of tugtupite—A new mineral, $Na_8Al_2Be_2Si_8O_{24}(Cl,S)_2$. *Acta Crystallogr.* **1966**, *20*, 812–816. [CrossRef]

90. Gaft, M.; Panczer, G.; Nagli, L.; Yeates, H. Laser-induced time-resolved luminescence of tugtupite, sodalite and hackmanite. *Phys. Chem. Mineral.* **2009**, *36*, 127–141. [CrossRef]

91. Finch, A.A.; Friis, H.; Maghrabi, M. Defects in sodalite-group minerals determined from X-ray-induced luminescence. *Phys. Chem. Mineral.* **2016**, *43*, 481–491. [CrossRef]

92. Povarennykh, A.S.; Platonov, A.N.; Tarashchan, A.N.; Belichenko, V.B. The colour and luminescence of Tugtupite (beryllosodalite) from Ilímaussaq, South Greenland. *GEUS Bull.* **1971**, *95*, 12.

93. Kendrick, M.A.; Jackson, M.G.; Hauri, E.H.; Phillips, D. The halogen (F, Cl, Br, I) and H_2O systematics of Samoan lavas: Assimilated-seawater, EM2 and high-[3]He/[4]He components. *Earth Planet. Sci. Lett.* **2015**, *410*, 197–209. [CrossRef]

94. Kendrick, M.A.; Honda, M.; Vanko, D.A. Halogens and noble gases in Mathematician Ridge meta-gabbros, NE Pacific: Implications for oceanic hydrothermal root zones and global volatile cycles. *Contrib. Mineral. Petrol.* **2015**, *170*, 43. [CrossRef]

95. Epp, T.; Marks, M.A.W.; Ludwig, T.; Kendrick, M.A.; Eby, N.; Neidhardt, H.; Oelmann, Y.; Markl, G. Crystallographic and fluid compositional effects on the halogen (Cl, F, Br, I) incorporation in pyromorphite-group minerals. *Am. Mineral.* **2019**, *104*, 1673–1688. [CrossRef]

96. Borst, A.M.; Friis, H.; Nielsen, T.F.D.; Waight, T.E. Bulk and mush melt evolution in agpaitic intrusions: Insights from compositional zoning in eudialyte, Ilímaussaq complex, South Greenland. *J. Petrol.* **2018**, *59*, 589–612. [CrossRef]

97. Pfaff, K.; Krumrei, T.; Marks, M.; Wenzel, T.; Rudolf, T.; Markl, G. Chemical and physical evolution of the 'lower layered sequence' from the nepheline syenitic Ilímaussaq intrusion, South Greenland: Implications for the origin of magmatic layering in peralkaline felsic liquids. *Lithos* **2008**, *106*, 280–296. [CrossRef]

98. Babiel, R.; Marks, M.A.W.; Neumann, U.; Markl, G. Sulfides in alkaline and peralkaline rocks: Textural appearance and compositional variations. *Neues Jahrb. Mineral. Abh. J. Mineral. Geochem* **2018**, *195*, 155–175. [CrossRef]

99. Graser, G.; Potter, J.; Köhler, J.; Markl, G. Isotope, major, minor and trace element geochemistry of late-magmatic fluids in the peralkaline Ilímaussaq intrusion, South Greenland. *Lithos* **2008**, *106*, 207–221. [CrossRef]

100. Hettmann, K.; Wenzel, T.; Marks, M.; Markl, G. The sulfur speciation in S-bearing minerals: New constraints by a combination of electron microprobe analysis and DFT calculations with special reference to sodalite-group minerals. *Am. Mineral.* **2012**, *97*, 1653–1661. [CrossRef]

101. Fleet, M.E.; Liu, X.; Harmer, S.L.; Nesbitt, H.W. Chemical state of sulfur in natural and synthetic lazurite by S K-edge xanes and X-ray photoelectron spectroscopy. *Can. Mineral.* **2005**, *43*, 1589–1603. [CrossRef]

102. Hassan, I. Transmission electron microscopy and differential thermal studies of lazurite polymorphs. *Am. Mineral.* **2000**, *85*, 1383–1389. [CrossRef]

103. Wulff-Pedersen, E.; Neumann, E.-R.; Burke, E.A.J.; Vannucci, R.; Bottazzi, P.; Ottolini, L.; Gjonnes, J.; Hansen, V. Origin and structural character of hauyne(ss) in spinel dunite xenoliths from La Palma, Canary Islands. *Am. Mineral.* **2000**, *85*, 1397–1405. [CrossRef]

104. Hassan, I.; Grundy, H.D. The crystal structures of sodalite-group minerals. *Acta Crystallogr. B Struct. Sci.* **1984**, *40*, 6–13. [CrossRef]

105. Giuseppetti, G.; Mazzi, F.; Tadini, C. The crystal structure of eudialyte. *Tschermaks Mineral. Petrogr. Mitt.* **1971**, *16*, 105–127. [CrossRef]

106. Johnsen, O.; Grice, J.D.; Gault, R.A. Kentbrooksite from the Kangerdlugssuaq intrusion, East Greenland, a new Mn-REE-Nb-F endmember in a series within the eudialyte group: Description and crystal structure. *Eur. J. Mineral.* **1998**, *10*, 207–219. [CrossRef]

107. Johnsen, O.; Grice, J.D. The crystal chemistry of the eudialyte group. *Can. Mineral.* **1999**, *37*, 865–891.

108. Sjöqvist, A.S.; Zack, T.; Honn, D.K.; Baxter, E.F. Modification of a rare-earth element deposit by low-temperature partial melting during metamorphic overprinting: Norra Kärr alkaline complex, southern Sweden. *Chem. Geol.* **2020**, *545*, 119640. [CrossRef]